

**Dynamic regulation of CFTR
chloride channel activity by PDZ-
based scaffolds**

Ji Hyun Lee

Department of Medical Science

The Graduate School, Yonsei University

**Dynamic regulation of CFTR
chloride channel activity by PDZ-
based scaffolds**

Directed by Professor Min Goo Lee

**The Doctoral Dissertation submitted to the
Department of Medical Science, the Graduate School
of Yonsei University in partial fulfillment of the
requirements for the degree of Doctor of Philosophy**

Ji Hyun Lee

December 2007

**The certifies that the Doctoral Dissertation
of Ji Hyun Lee is approved**

Thesis Supervisor: Min Goo Lee

Thesis Committee Member: Jeung-Gweon Lee

Thesis Committee Member: Joo-Heon Yoon

Thesis Committee Member: Man Wook Hur

Thesis Committee Member: Dong-Min Shin

**The Graduate School
Yonsei University**

December 2007

ACKNOWLEDGEMENTS

제가 이곳 약리학교실과 인연을 맺은 지 벌써 6년이란 시간이 흘렀습니다. 학부 4학년 때 유학을 갈지 아니면 취직을 할지 아직 무엇을 해야 할지 정하지 못해서 고민하고 있을 때 우연히 남궁완 선배를 따라서 이곳 약리학교실에 왔다가 지금 제 지도교수님이신 이민구 교수님께 인사만 드리려고 했는데 “언제부터 나올 수 있지?” 라는 한마디에 4학년 2학기 때부터 학부 수업을 마치면 곧장 이곳 약리학교실에 와서 실험을 배우면서 자연스럽게 석사과정에 입학하였습니다. 힘들었지만 참 즐거웠던 2년의 석사과정을 마치고 여기서 박사를 할지 아니면 유학을 갈지 또 한번 고민을 할 때 이민구 교수님께서 이렇게 말씀을 하셨습니다. “석사만 하면 진정한 선생님 학생이 아니고 박사를 해야 진정한 선생님 학생이다” 라고. 이렇게 저는 또 이곳 약리학교실 박사과정에 입학하였고 4년이란 시간 동안의 제 연구 결과를 박사학위 논문으로 정리하려고 합니다. 돌이켜보면 이곳 약리학교실에서 6년이란 시간은 제 20대의 반을 보낸 길고도 짧은 시간이었고, 주위에 많은 고마운 분들이 있었기에 지금의 제가 있을 수 있었습니다.

제일 먼저 제 지도교수님이신 이민구 교수님께 감사하다는 말을 전하고 싶습니다. 워낙 말이 없으셔서 처음에는 너무나 어려운 교수님이셨지만 처음부터 저와의 인연을 소중히 생각하셨고 저에게 과학자로서의 사고 방식과 마음가짐을 가르쳐 주신 참 좋으신 분이셨습니다. 그리고 지금은 우리 곁을 떠났지만 친 할아버지처럼 따뜻하게 반겨주셨던 이우주 교수님, 항상 존재감만으로도 너무나도 든든하고 더 열심히 연구하라고 가끔 맞난 것도 사주시는 김경환 교수님, 지금 대회협력 본부장이셔서 너무나도 바쁘시고 또 마라톤을 좋아하시는 멋진 안영수 교수님, 우리 교실 주임교수님이시고 항상 웃는 얼굴로 따뜻하게 대하여 주시는 김동구 교수님, 멋진 이력을 갖고 계시고 현재 우리 학교 임상시험센터를 이끌고 계신 박경수 교수님, 교수님이시지만 아직도 가방을

메고 다니셔서 젊음과 열정이 느껴지는 김철훈 교수님, 그리고 지금은 본교 식품영양학과로 자리를 옮기셨지만 항상 세심하게 챙겨주셨던 김혜영 교수님, 처음엔 선배로 인연을 시작하였지만 지금은 교수님이 되셔서 나의 본보기가 되는 김주영 교수님, 언제나 아침 일찍 오셔서 열심히 연구하는 열정적인 연구자의 모습을 보여주신 임주현 교수님께 진심으로 감사드립니다.

또한 아직 많이 부족한 저에게 자문기간 동안 항상 많이 칭찬해 주셨던 이정권 교수님, 그리고 자문위원이시기 이전부터 저에게 많은 격려와 관심을 가져주셨던 윤주현 교수님, 보다 좋은 학위 논문이 될 수 있도록 학위 논문을 꼼꼼히 검토해 주시고 많은 자문을 해 주신 허만옥 교수님, 자문기간 동안 바쁘신데도 항상 제일 먼저 챙겨주신 신동민 교수님께도 진심으로 감사드립니다.

즐겁고 힘들었던 시간을 늘 함께한 실험실 식구들 저에게는 참 든든한 동반자였습니다. 나와 이곳 약리학교실과의 인연을 만들어 주었고 언제나 나에게 따뜻했던 완선배, 아직도 가끔 전화해서 실험실 소식을 묻는 민재오빠, 아직 많은 것을 모르는 나에게 항상 충고를 아끼지 않는 우인선배, 항상 즐거운 이야기로 우리를 웃겼던 씨니언니, 선배로써 좀더 잘해주지 못해서 항상 미안한 요셉이와 승근이 모두 이곳 약리학교실을 떠났지만 진심으로 감사하다는 말을 전합니다.

오빠라고 부르면서 좀더 친하게 지내고 싶었지만 그러지 못해서 너무나도 아쉬운 이성희 선생님, 매사 너무나도 열심히 생활해서 항상 나를 돌아보게 만드는 현영오빠, 후배이지만 가끔은 나의 고민을 들어주는 든든한 현우, 넓은 마음을 가졌고 우리 연구실 안주인 정남누나, 항상 매사 열심히 하고 지금 치프로서 우리 랩을 이끌고 있는 재석이, 성격이 쿨한 이정수 선생님, 우리 랩 막내 우영이, 포스트닥으로 새롭게 우리 랩에 합류한 광진오 선생님께도 감사합니다.

그리고 내가 아무리 괴롭혀도 항상 웃는 얼굴로 잘 설명해 주셨던 이진우 선생님, 아니 지금은 이진우 교수님, 언제나 열심히 연구하는 이정호 선생님, 고향이 같아서 친근한 기호, 나를 너무나도 잘 따라서 친동생 같은 우리,

예쁘고 터프한 재현이, 요즘 실험이 많아서 조금 힘들어 보이는 미경이, 조용조용 열심히 하는 영신이, 참 성격이 좋고 열심히 하는 복이, 좀더 잘 먹고 살이 썩어야 하는 이쁜이 효선이, 그리고 임상시험센터에 있어서 많이 볼 수 없어서 아쉬운 윤정리와 아영 선생님, 항상 따뜻한 말을 건네는 주경돈 선생님, 잠시 떠났다가 다시 교실로 돌아온 순옥리와 동휘, 지금 본교 식품영양학과로 자리를 옮겨서 자주 볼 수 없어서 아쉬운 정혜연 선생님과 서정연 선생님.. 모두 감사합니다. 그리고 이번에 같이 졸업하는 인숙언니, 이장원 선생님, 보람이 모두 수고 많았습니다. 언제나 약리학교실을 지켜주시고 참 순수하고 따뜻한 마음을 가진 선혜언니, 맥가이버처럼 무슨 일이든 척척 해결해 주시는 멋쟁이 임종수 선생님, 그리고 김건태 선생님께도 감사의 말을 전합니다.

힘들고 지칠 때 위로가 되어준 네 소중한 친구 홍은이, 회원이, 드디어 좋은 짝은 만나 곧 장가 가는 나를 가장 잘 이해해 주었고 챙겨주었던 친구 정효, 그리고 3년 동안 기숙사 생활을 같이 해서 항상 편하고 든든한 내 고등학교 동기들, 후배이지만 항상 나를 챙겨준 세희, 항상 힘내라고 맛난 것을 사준 정현선배, 그리고 후배 민희, 용식에게게 진심으로 감사의 마음을 전합니다.

끝으로 지금까지 저를 키워주시고 늘 마음속의 큰 나무가 되어주시는 부모님께 진심으로 감사드립니다. 그리고 누구보다도 나를 아껴주고 같이 다니면 가끔 남자친구로 오인 받는 하나밖에 없는 우리 오빠에게도 감사의 마음을 전합니다.

TABLE OF CONTENTS

ABSTRACT	1
I. INTRODUCTION	3
II. MATERIALS AND METHODS	5
1. Cell Cultures and Plasmid Vectors	5
2. Surface Plasmon Resonance (SPR) Measurements and Kinetic Analysis of Sensorgrams	5
3. Measurements of Cl⁻ Channel Activities	6
4. Reverse Transcription-PCR	8
5. Immunoprecipitation and Immunoblotting	8
6. GST Pulldown Assay	9
7. Immunohistochemistry	10
8. Measurements of PDE Activity	10
III. RESULTS	12
1. Shank2 and EBP50 Compete for Binding on CFTR	12
2. Regulation of CFTR Cl⁻ Channel Activity by CFTR-EBP50 and CFTR-Shank2 Competitions	14

3. Shank2 Associates with PDE4D	16
4. Shank2 and PDE4D Associate in Vivo	22
IV. DISCUSSION	25
V. CONCLUSION	29
REFERENCES	30
ABSTRACT (IN KOREA)	34
PUBLICATION LIST	36

LIST OF FIGURES

- FIGURE 1. Interactions between CFTR and PDZ-based adaptors determined by surface plasmon resonance (SPR) assays ----- 13**
- FIGURE 2. Regulation of CFTR single channel activity by a competition between CFTR-EBP50 and CFTR-Shank2 PDZ binding ----- 15**
- FIGURE 3. Shank2 associates with PDE4D ----- 18**
- FIGURE 4. Domains responsible for the association between Shank2 and PDE4D ----- 21**
- FIGURE 5. Shank2 and PDE4D associate in vivo ----- 23**
- FIGURE 6. A model for the regulation of CFTR through interaction with EBP50 and Shank2 ----- 27**

ABSTRACT

Dynamic regulation of CFTR chloride channel activity by PDZ-based scaffolds

Ji Hyun Lee

Department of Medical Science

The Graduate School, Yonsei University

(Directed by Professor Min Goo Lee)

Disorganized ion transport caused by hypo- or hyper-functioning of the cystic fibrosis transmembrane conductance regulator (CFTR) can be detrimental and may result in life-threatening diseases such as cystic fibrosis or secretory diarrhea. Accordingly, CFTR is controlled by elaborate positive and negative regulations for an efficient homeostasis. It has been shown that expression and activity of CFTR can be regulated either positively or negatively by PDZ (PSD-95/discs large/ZO-1) domain-based scaffolds. Although a positive regulation by PDZ domain-based scaffolds such as EBP50/NHERF1 is established, the mechanisms for negative regulation of the CFTR by Shank2, as well as the effects of multiple scaffold interactions, are not known. Therefore, I demonstrated a physical and physiological competition between EBP50-CFTR and Shank2-CFTR associations and the dynamic regulation of CFTR activity by these positive and negative interactions using the surface plasmon resonance

assays and patch clamp experiments. Furthermore whereas EBP50 recruits a cAMP-dependent protein kinase (PKA) complex to CFTR, Shank2 was found to be physically and functionally associated with the cyclic nucleotide phosphodiesterase PDE4D that precludes cAMP/PKA signals in epithelial cells and mouse brains.

These findings strongly suggest that balanced interactions between the membrane transporter and multiple PDZ-based scaffolds play a critical role in the homeostatic regulation of epithelial transport and possibly the membrane transport in other tissues.

Key Word: Cystic Fibrosis Transmembrane Conductance Regulator (CFTR), PDZ-based scaffolds, EBP50, Shank2, PDE4, cAMP

**Dynamic regulation of CFTR chloride channel activity
by PDZ-based scaffolds**

Ji Hyun Lee

*Department of Medical Science
The Graduate School, Yonsei University*

(Directed by Professor Min Goo Lee)

I. INTRODUCTION

CFTR is a Cl⁻ channel and the key regulator of fluid and ion transport in the gastrointestinal, respiratory, and genitourinary epithelia¹. Hypo-functioning of CFTR due to genetic defects causes cystic fibrosis, the most common lethal genetic disease in Caucasians^{2,3}, whereas hyper-functioning of CFTR resulting from various infections evokes secretory diarrhea⁴, the world's leading cause of mortality in early childhood (<http://www3.who.int/whosis>). Therefore, maintaining and regulating a dynamic balance between CFTR-activating and CFTR-inactivating machineries is an important mechanism for maintaining body homeostasis.

Accumulating evidence suggests that protein-protein interactions play a critical role in the regulation of CFTR and other epithelial transporters^{5,6}. PDZ (PSD-95/discs large/ZO-1)-based scaffolds, best studied in the post-synaptic density (PSD) region of neurons, have emerged as a large group of proteins that sequester functionally-related groups of transporters, receptors, and other

effector proteins into integrated molecular complexes⁷. Epithelial cells also utilize specific PDZ proteins to direct the polarized activities in their apical and basolateral membranes. Previous reports described that functional and physical associations between the PDZ domain-containing protein Shank2 and two epithelial transporters, the cystic fibrosis transmembrane conductance regulator (CFTR) and the Na⁺/H⁺ exchanger 3 (NHE3)^{8,9}. Interestingly, Shank2 attenuated the cAMP-dependent regulation of CFTR and NHE3. Conversely, it has been shown that PDZ-based scaffolds, such as EBP50/NHERF1 and E3KARP/NHERF2, can enhance the effects of cAMP on these transporters by recruiting a cAMP-dependent protein kinase anchoring protein (AKAP)/PKA complex^{10,11}.

The PDZ domain of Shank proteins has a three-dimensional structure very similar compared to the PDZ domains of EBP50/NHERF1. In particular, these PDZ domains all contain a negatively-charged amino acid at the end of the β C strand of the PDZ domain structures (Glu⁴³ in hEBP50, Asp⁶³⁴ in rShank1, and Asp⁸⁰ in hShank2)¹², which preferentially interacts with a positively-charged residue at the -1 position in the C-terminus of the membrane transporters, such as -TRL in CFTR. Therefore, the question arises whether EBP50 and Shank2 have distinct CFTR binding sites or mutually compete for binding of a single site in cells expressing both adaptor proteins. In the present study, I determined the kinetic properties and physiological significance of the interactions between CFTR and the PDZ-based adaptors, EBP50 and Shank2.

II. MATERIALS AND METHODS

1. Cell Cultures and Plasmid Vectors

NIH 3T3 and COS7 cells were maintained in Dulbecco's modified Eagle's medium supplemented with 10% fetal calf serum. T84 cells were purchased from the American Type Culture Collection (ATCC CCL-248) and maintained in a 1:1 mixture of Ham's F-12 medium and Dulbecco's modified Eagle's medium supplemented with 5% fetal bovine serum. CHO-K1 cells (KCLB 10061; Korea Cell Line Bank, Seoul, Korea) were maintained in RPMI 1640 medium supplemented with 10% fetal bovine serum. The pcDNA3.1-rShank2/CortBP1¹³, pcDNA3.1-hEBP50/NHERF-1⁸, and pCMV5 vectors containing rPDE4D1 to rPDE4D9 have been described previously¹⁴.

2. Surface Plasmon Resonance (SPR) Measurements and Kinetic Analysis of Sensorgrams

PDZ1 (1-139), PDZ2 (132-299), and PDZ1+2 (1-299) domains of hEBP50/NHERF1 and the PDZ domain of rShank2/CortBP1 (1-142) were PCR-amplified and cloned into the pRSET A vector (Life Technologies Inc., Gaithersburg, MD) to create His-tagged constructs. C-terminal 29 aa residues of hCFTR ([NM_000492](#)) and PDZ1+2 of hEBP50 were PCR-amplified and cloned into the pGEX-4T-1 vector (Amersham Biosciences, Piscataway, NJ) to create GST-fusion constructs. All constructs were confirmed by sequence analysis. All fusion proteins were expressed in *E. coli* BL21 (DE3) cells and purified on Ni²⁺-nitrilotriacetic acid (NTA) resin (Qiagen, Venlo, The Netherlands) and glutathione-Sepharose 4B (Amersham Biosciences), as appropriate. The

purified proteins were quantified using Bio-Rad protein assay reagent, and their purity was assessed as >90% by Coomassie staining of SDS-PAGE gels. An SPR system equipped with an NTA chip (BIAcore 3000; Biacore AB, Uppsala, Sweden) was used to capture His-tagged PDZ fusion proteins. Analytes (GST-tagged proteins) at various concentrations in HEPES-buffered saline-EP (0.01 M Hepes, 0.15 M NaCl, 50 μ M EDTA, 0.005% Tween20, pH 7.4) were perfused at a flow rate of 30 μ l/min. The sensor chip was regenerated between each analysis using successive injections of solutions containing 0.15 M NaCl and 0.35 M EDTA. Response curves were generated by subtracting the background signal generated simultaneously by the control flow cell. Background-subtracted curves were prepared for fitting by subtracting the signal generated by buffer alone on experimental flow cells. Sensorgram curves and kinetic parameters were evaluated by the BIAEVALUATION 3.1 software (Biacore AB), which uses numerical integration algorithms.

3. Measurements of Cl⁻ Channel Activities

Whole-cell recordings were performed on CFTR transfected CHO-K1 cells. The pipette solution contained (in mM) 140 N-methyl D-glucamine chloride (NMDG-Cl), 5 EGTA, 1 MgCl₂, 1 Tris-ATP, and 10 HEPES (pH 7.2), and the bath solution contained 140 NMDG-Cl, 1 CaCl₂, 1 MgCl₂, 10 Glucose, and 10 HEPES (pH 7.4). All experiments were performed at room temperature (22-25 °C). Pipettes were pulled from borosilicate glass and had resistances of 3-5 M Ω after fire polishing. Seal resistances were typically between 3-10 G Ω . After establishing the whole-cell configuration, CFTR was activated by adding

forskolin and/or IBMX. The holding potential used was -30 mV and the current output was filtered at 5 kHz. Currents were digitized and analyzed using an AxoScope 8.1 system and a Digidata 1322A AC/DC converter (Axon Instruments, Union City, CA).

Single channel activity of CFTR was measured in inside-out configurations using fire-polished pipettes with a resistance of 20-25 M Ω . The pipette solution contained (in mM) 140 NaCl, 5 KCl, 1 MgCl₂, 1 CaCl₂, and 10 HEPES (pH 7.2), and the bath solution contained 140 NaCl, 5 KCl, 1 MgCl₂, and 10 HEPES (pH 7.4). Following patch excision, channels were activated by adding the catalytic subunit of PKA (40 unit/ml; Promega, Madison, WI) and 1 mM MgATP. After channel activation, EBP50 and/or Shank2-PDZ at desired concentrations were added to the bath. Holding voltage used in the single channel recording was +60 mV. The pCLAMP software package (version 9.2, Axon Instruments) was used for data acquisition and analysis. The voltage and current data were low-pass filtered at 1 kHz during the recordings and the single channel data were further digitally filtered at 25 Hz. Channel open probability (P_o) was estimated using the following equation:

$$P_o = \sum_{i=1}^N t_i / TN$$

where t_i is the time spent above a threshold set at 0.5 times channel current amplitude, T is the duration of the recording, and N is the number of channels in patch. The number of active channels in a patch was determined from the number of simultaneously open channels during at least 15 min of recording.

4. Reverse Transcription-PCR

RT-PCR analysis was performed to identify the PDE isoforms in NIH 3T3 cells and T84 cells. The primer sequences specific to PDE3 and PDE4 were selected from regions common to both mouse and human PDEs: 1) PDE3A, sense (5'-CAC AGG GCC TTA ACT TAC AC-3'), antisense (5'-TTG AGT CCA GGT TAT CCA TGA C-3'), PCR product 370 bp; 2) PDE3B, sense (5'-CAG GAA GGA TTC TCA GTC AGG-3'), antisense (5'-GTC ATT GTA TAA AAC TGC CTG AGG-3'), PCR product 464 bp; 3) PDE4A, sense (5'-ATC AAC ACC AAT TCG GAG C C-3'), antisense (5'-TCA CCC TGC TGG AAG AAC TC-3'), PCR product 398 bp; 4) PDE4B, sense (5'-AGT CCT TGG AAT TGT ATC GG-3'), antisense (5'-CTG GAT CAA TCA CAC AAA GCG TC-3'), PCR product 432 bp; 5) PDE4C, sense (5'-TTC CAG ATC CCA GCA GAC AC-3'), antisense (5'-ATG ACC ATC CTG CGC AGA CTC-3'), PCR product 392 bp; 6) PDE4D, sense (5'-GCC AAG GAA CTA GAA GAT GTG-3'), antisense (5'-CAT CAT GTA TTG CAC TGG C-3'), PCR product 328 bp.

5. Immunoprecipitation and Immunoblotting

CHO-K1, COS-7, T84 cells, and rat cerebellum were lysed with lysis buffer (20 mM HEPES pH 7.4, 200 mM NaCl, 5 mM EDTA, 1% Triton X-100, 1 mM NaVO₄, 1 mM β-glycerophosphate) containing complete protease inhibitor mixture (Roche Applied Science, Mannheim, Germany). After lysis, cell debris was removed by centrifugation, and cleared lysates were mixed with the appropriate antibodies and incubated overnight at 4 °C. Immune complexes were collected by incubation for 2 h at 4 °C with protein A/G PLUS agarose and

washed four times with lysis buffer prior to electrophoresis. The immunoprecipitates and cell lysates were suspended in 2x SDS sample buffer and boiled for 5 min and then separated by SDS-PAGE. The separated proteins were transferred to nitrocellulose membranes, and the membranes were blocked by incubation for 1 h in a solution containing 5% nonfat dry milk in 20 mM Tris-HCl, pH 7.5, 150 mM NaCl, and 0.05% Tween 20. The membranes were then incubated with the appropriate primary and secondary antibodies, and protein bands were detected with enhanced chemiluminescence solutions. Rabbit polyclonal antibodies anti-Shank2 1136, anti-PDE4D5 α -4D5, and the mouse monoclonal PAN-PDE4D antibody, M3S1 were described previously. Rabbit polyclonal PAN-PDE4D antibody, ab14613, was purchased from Abcam Inc., Cambridge, UK.

6. GST Pulldown Assay

Regions corresponding to residues of rShank2 PDZ (1-142), PR (134-1176), and SAM (1164-1253) domains were PCR-amplified and cloned into pGEX-4T-1 vector (Amersham Biosciences) to create GST-fusion constructs. Shank2 PR domains were further dissected and two GST-fusion constructs were generated; PR1 (134-669) and PR2 (647-1176). All fusion proteins were expressed in *E. coli* BL21 (DE3) and purified with glutathione-Sepharose 4B (Amersham Biosciences). For pull-down assays, CHO cells were lysed on ice in a 1% Triton X-100 buffer containing 150 mM NaCl, 2 mM MgCl₂, 2 mM CaCl₂, 10 mM HEPES pH 7.4 and proteinase inhibitors (CompleteMini, Roche). Debris was removed by centrifugation and 100 μ l of lysate supernatants was

supplemented with 900 μ l of buffer prior to addition of 10 μ g of each GST fusion protein. Following overnight incubation at 4 °C, samples were supplemented with 80 μ l of glutathione–Sepharose (Amersham Biosciences) and incubated for an additional 4 h at 4 °C. The glutathione–Sepharose was pelleted and washed (3 x 5 min) at 4 °C with wash buffer (PBS containing 0.1% Triton X-100 and 100 mM β -mercaptoethanol) prior to resuspension in SDS sample buffer and SDS–PAGE.

7. Immunohistochemistry

Colon tissues from Sprague-Dawley rats were embedded in OCT (Miles, Elkhart, IN), frozen in liquid N₂, and cut into 4- μ m sections. The sections were fixed and permeabilized by incubation in cold methanol for 10 min at 20 °C. Nonspecific binding sites were blocked by incubation for 1 h at room temperature with 0.1 ml of phosphate-buffered saline containing 5% goat serum, 1% bovine serum albumin, and 0.1% gelatin (blocking medium). After blocking, the sections were stained by incubation with polyclonal anti-Shank2 1136 and monoclonal anti-pan PDE4D M3S1 antibodies, followed by appropriate secondary antibodies tagged with fluorophores. Images were obtained with a Zeiss LSM 510 confocal microscope.

8. Measurements of PDE Activity

Whole brain tissues from wild type and PDE4D knock-out mice were lysed in buffer containing 50 mM HEPES, pH 7.4, 250 mM NaCl, 10% glycerol, 0.5% Nonidet P-40, 1 mM EDTA, 0.2 mM EGTA, 10 mM NaF, 10 mM Na₄P₂O₇,

1 μM microcystin, 2 mM 4-(2-aminoethyl) benzenesulfonylfluoride, and a mixture of protease inhibitors. Cell lysates were spun at 14,000 x g, and supernatants were immunoprecipitated using 5 μl of anti-Shank2 antibody coupled to 25 μl of protein G sepharose for 4 h. After centrifugation, pellets were washed three times and PDE activity was then measured. In brief, samples were assayed in a reaction mixture of 200 μl containing 40 mM Tris-HCl, pH 8.0, 10 mM MgCl_2 , 5 mM β -mercaptoethanol, 1 μM cAMP, 0.75 mg/ml bovine serum albumin, and 0.1 μCi of [^3H]cAMP for 10 min at 33 $^\circ\text{C}$. The reaction was terminated by the addition of 200 μl of 10 mM EDTA in 40 mM Tris-HCl, pH 8.0, followed by heat inactivation in a boiling water bath for 1 min. The PDE reaction product 5'-AMP was then hydrolyzed by incubation of the assay mixture with 50 μg of *Crotalus atrox* snake venom for 20 min at 33 $^\circ\text{C}$. The resulting adenosine was separated by anion exchange chromatography using 1 ml of AG1-X8 resin and quantitated by scintillation counting.

III. RESULTS

1. Shank2 and EBP50 Compete for Binding on CFTR

To understand the dynamics of CFTR positive and negative regulations, I determined the binding kinetics of the association between CFTR and the PDZ domains of EBP50 and Shank2 using SPR analyses (FIG. 1). As EBP50 has two PDZ domains, three His-tagged proteins, PDZ1 (1-139), PDZ2 (132-299), and PDZ1+2 (1-299), were used in order to analyze their kinetics separately. His-tagged PDZ domains were captured on NTA chips, and their binding to the GST-tagged C-terminus of CFTR was sensed by SPR. As shown in the sensorgrams, the PDZ domains of Shank2 and EBP50 specifically bind the C-terminus of CFTR in a dose-dependent fashion (FIG. 1, a and b). The overall dissociation constants at the equilibrium state (KDs) of Shank2 PDZ and EBP50 PDZ1+2 were within comparable ranges at the tens of nanomolar levels (FIG. 1c). Interestingly, EBP50 PDZ1+2 has approximately a one order of magnitude faster association (K_a) and dissociation (K_d) kinetics than Shank2 PDZ. Further analyses of EBP50 PDZs using separate PDZ1 and PDZ2 proteins revealed that the overall EBP50 binding to CFTR is driven by PDZ1, which has a ~3 times higher affinity than PDZ2 (FIG. 1c). A solution competition assay was performed to examine the possibility of mutual competition between the PDZs of Shank2 and EBP50 in binding to CFTR. After capturing His-tagged Shank2 PDZ on NTA chips, the SPR system was perfused with a fixed dose of the C-terminus of CFTR (300 nM) and increasing doses of GST-tagged EBP50 PDZ1+2. Importantly, the addition of EBP50 PDZs dose dependently decreased the association between Shank2 PDZ and CFTR with an IC_{50} value of 91nM (FIG. 1d).

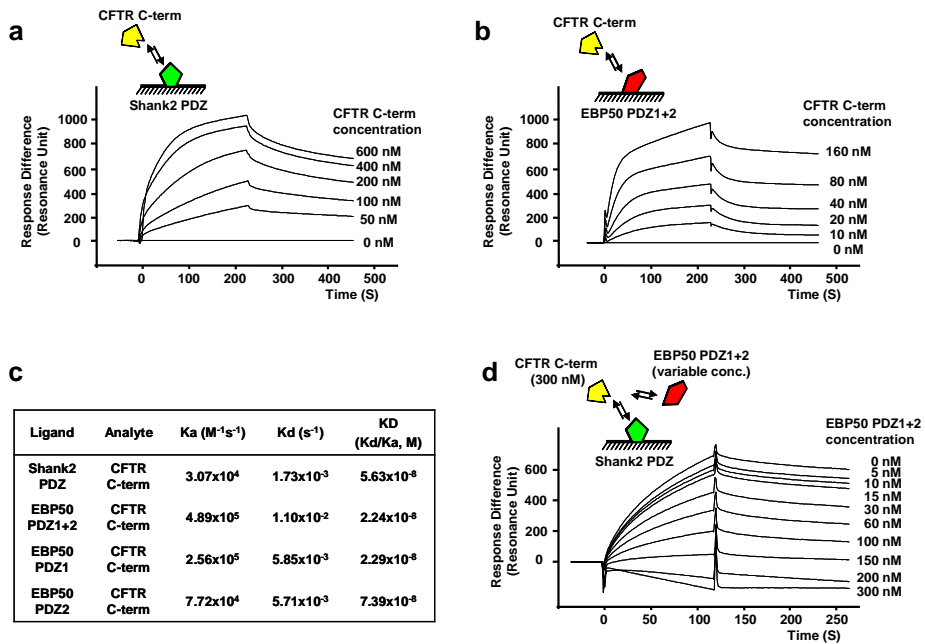


FIGURE 1. Interactions between CFTR and PDZ-based adaptors determined by surface plasmon resonance (SPR) assays (a, b) Sensorgrams showing the interaction between the C-terminus of CFTR and the PDZ domains of Shank2 and EBP50/NHERF1. His-tagged PDZ domains of Shank2 and EBP50 were captured on nitrilotriacetic acid (NTA) chips which were then perfused with various concentrations of a peptide encoding the C-terminal 29 aa of CFTR. (c) Binding kinetics of the interaction between CFTR and the PDZ domains of Shank2 and EBP50. Values shown represent the average of two experiments each performed in duplicate. (d) Sensorgram of a solution competition assay between CFTR-Shank2 PDZ and CFTR-EBP50 PDZ1+2 interactions. After capturing His-tagged Shank2 PDZ, the NTA chips were perfused with a fixed concentration of the C-terminus of CFTR (300 nM) and increasing concentrations of the GST-tagged EBP50 PDZ1+2. EBP50 PDZ1+2 dose-dependently decreased the CFTR-Shank2 PDZ association with an IC₅₀ value of 91 nM (n=3). K_a: association constant, K_d: dissociation constant, K_D: overall dissociation constant at equilibrium status (K_d/K_a).

2. Regulation of CFTR Cl⁻ Channel Activity by CFTR-EBP50 and CFTR-Shank2 Competitions

The above results imply that Shank2 and EBP50 compete for binding on CFTR. This competitive balance may affect CFTR ion transporting activities at the apical membrane of intestine, pancreas, and kidney epithelia where Shank2 and EBP50 are abundantly expressed^{6,8}. Therefore, I determined the effects of the competition between EBP50 and Shank2 PDZ binding on the CFTR Cl⁻ channel activity using inside-out configurations (FIG. 2). Following patch excision from CFTR-transfected CHO cells, patch membranes were washed with a high bath flow for 5 min to eliminate endogenous activation. When CFTR was activated by the addition of the catalytic subunit of PKA and ATP to the bath solution, an ion channel activity with a single channel conductance of 7.1 ± 0.3 pS and a linear I-V relationship was evoked, which was absent in mock-transfected cells. It has been shown that scaffolds with multiple PDZ domains, such as EBP50 and CAP70/PDZK1, can activate CFTR Cl⁻ channel activity independent of cAMP signals by altering protein conformation including multimerization^{15,16}. In agreement with these reports, treatment with EBP50 (100 nM) induced a 2.8-fold increase in the open probability (P_o) of CFTR. Importantly, addition of Shank2 PDZ (300 nM) inhibited the EBP50-induced increase in CFTR P_o by $75 \pm 8\%$ (FIG. 2, a and c). The effect of Shank2 PDZ versus EBP50 competition was then examined in reverse order. Shank2 PDZ treatment alone did not evoke significant changes in CFTR P_o at basal levels however it greatly inhibited the CFTR activation mediated by EBP50. Addition of EBP50 induced only a minor increase in CFTR P_o after Shank2 pre-treatment (FIG. 2, b and d). When performing the

above experiments using EBP50 PDZ1+2 which does not bind AKAPs due to the lack of the ERM domain, I obtained results similar to those using the entire EBP50 protein (FIG. 2, c and d).

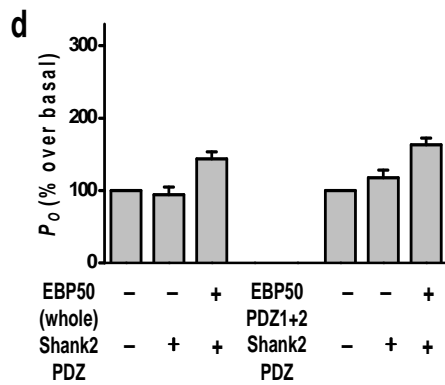
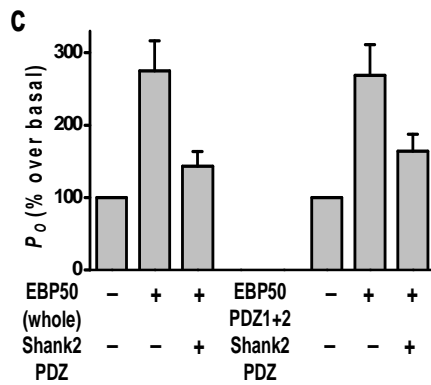
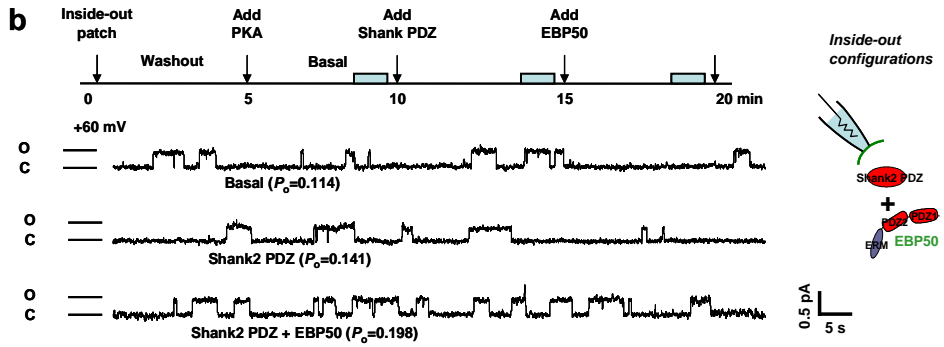
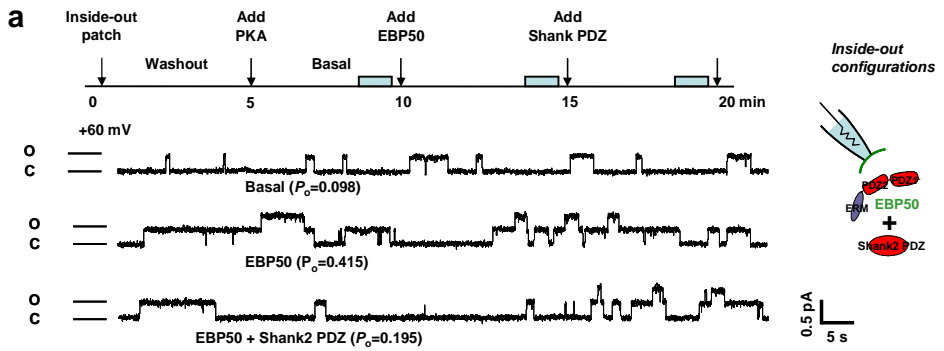
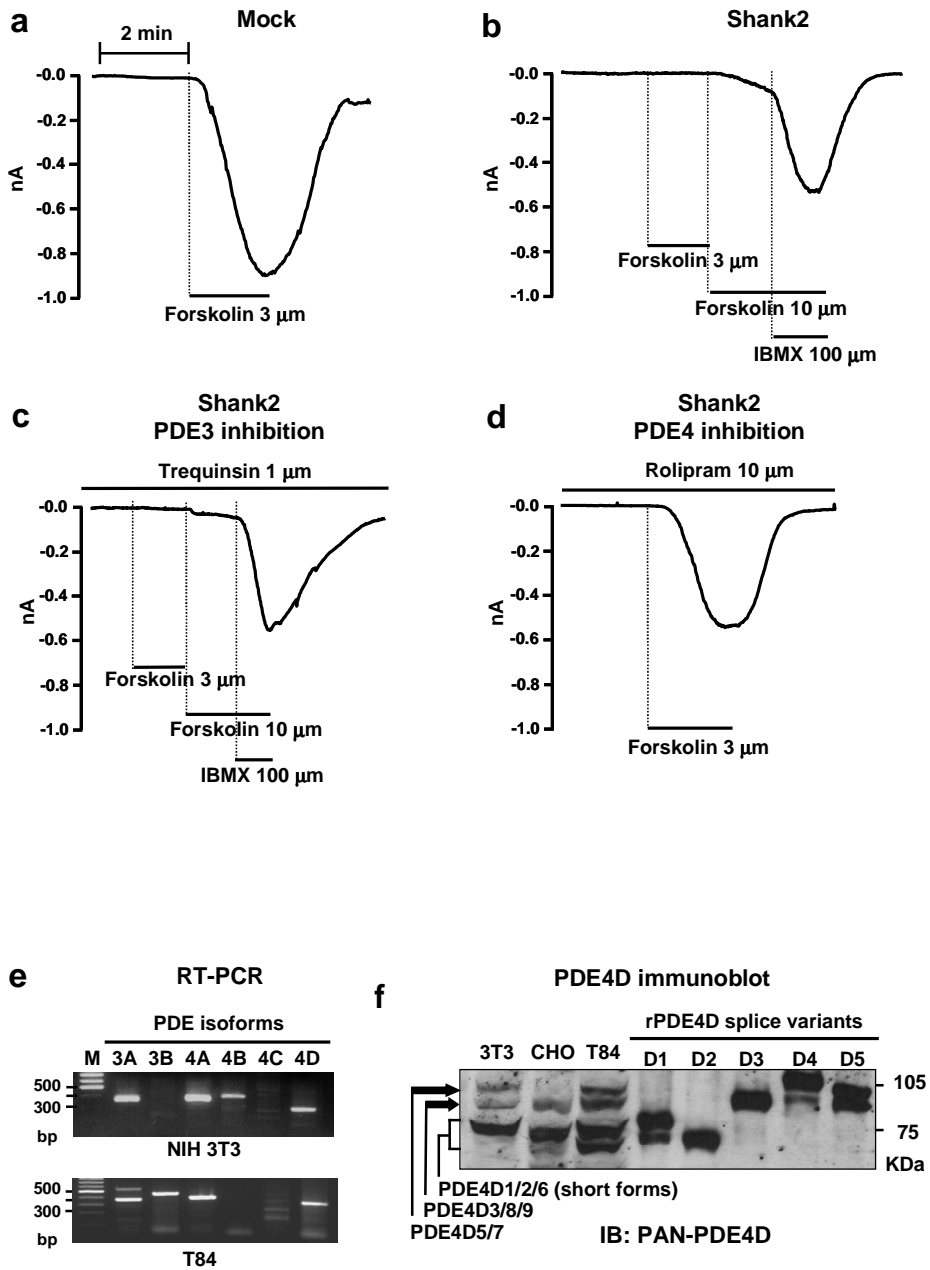


FIGURE 2. Regulation of CFTR single channel activity by a competition between CFTR-EBP50 and CFTR-Shank2 PDZ binding CFTR Cl⁻ channel activity was measured in CFTR-transfected CHO cells with inside-out configurations. Current records at +60 mV were analyzed to estimate the open probability (P_o) (a) After a 5-min wash of patch membranes, CFTR was activated by addition of PKA. Solutions containing EBP50 (100 nM) with and without Shank2 PDZ (300 nM) were perfused to the bath chamber at 5-min intervals. P_o was calculated from the recording of the last 1 min of each 5 min interval. Similar experiments were performed with EBP50 PDZ1+2, which lacks the AKAP/PKA-binding ERM domain, instead of EBP50 (whole). A summary of five experiments with EBP50 and three experiments with EBP50 PDZ1+2 is presented in panel c. (b) The effect of Shank2 PDZ and EBP50 binding on CFTR activity was examined in reverse order of panel a, with Shank2 PDZ treatment preceding the EBP50 treatment. A summary of five experiments with EBP50 and three experiments with EBP50 PDZ1+2 is presented in panel d.

3. Shank2 Associates with PDE4D

An important clue was obtained in an experiment with the nonselective PDE inhibitor, 3-isobutyl-1-methylxanthine (IBMX) (FIG. 3, a-d). Stimulation of CFTR-expressing CHO cells with 3 μ M forskolin induced a CFTR Cl^- current that is dependent on the presence of Cl^- in bath and pipette solutions, is inhibited by 5-nitro-2-(3-phenylpropylamino)benzoate, and has linear I-V relationships in whole-cell configurations. However, when Shank2 was co-expressed, the same amount of forskolin produced very small, or no CFTR currents. Interestingly, additional treatment with IBMX evoked a robust CFTR current in Shank2-expressing cells, although its peak amplitude was still $56 \pm 7\%$ that of mock-transfected cells (FIG. 3, a and b). These results suggest a functional association between the PDE activity and the Shank2-mediated inhibition of CFTR. Next I identified the PDE subtypes involved, and determined whether Shank2 directly interacts with PDEs. Of the 11 PDE families, PDE3 and PDE4 are strong candidates for Shank2-association as they are sensitive to IBMX and are known to be expressed in epithelial cells¹⁷. The PDE3 family consists of two genes, 3A and 3B, and the PDE4 family of four, 4A - 4D. RT-PCR results using primers specific to the common regions of mouse and human PDEs revealed that several PDE3 and PDE4 genes, including PDE3A, 4A, and 4D, are expressed in mouse fibroblast NIH 3T3 cells and human colonic T84 cells (FIG. 3e). As both PDE3 and PDE4 are expressed, the patch clamp experiment shown in FIG. 3b was repeated after pretreatment of the cells with the PDE3-specific inhibitor, trequinsin and the PDE4-specific inhibitor, rolipram (FIG. 3, c and d). PDE3 inhibition did not alter the effects of

Shank2 (FIG. 3c). Conversely, when PDE4 was inhibited by rolipram, 3 μ M forskolin consistently induced a robust CFTR current in Shank2-expressing cells (FIG. 3d, n=5), strongly suggesting an association between Shank2 and PDE4 isoforms. Recently, two reports suggested that PDE4D plays a major role in forming a cAMP diffusion barrier at the apical regions of epithelial cells^{18,19}. Consistent with this notion, expression of PDE4D proteins was observed in the immunoblots of NIH 3T3, CHO, and T84 cells (FIG. 3f) in which the inhibitory effects of Shank2 on cAMP/PKA signals were demonstrated in this and previous studies^{8,9}. To probe for a physical association between Shank2 and PDE4D, coimmunoprecipiations(co-IPs) were performed. Human and rat PDE4D loci have multiple transcriptional units that code for at least 9 splice variants, PDE4D1 to PDE4D9¹⁴. Among them, PDE4D5 has been shown to be expressed in epithelial cells and to mediate cAMP hydrolysis at the apical microdomain¹⁸. Thus, Shank2 and the PDE4D splice variant, PDE4D5, were overexpressed in CHO cells followed by IP with antibodies against Shank2 and PDE4D5 (FIG. 3g). Shank2 proteins were observed in immunoprecipitates with PDE4D5-specific antibodies. In a converse experiment, PDE4D5 could be detected in Shank2 immunoprecipitates. These co-IPs were specific as they could only be detected in cells expressing both Shank2 and PDE4D5 (FIG. 3g).



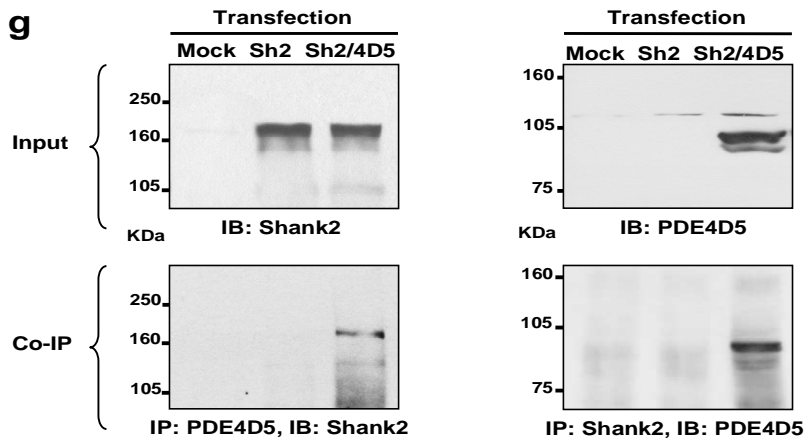


Figure 3. Shank2 associates with PDE4D (a-d) CFTR Cl⁻ channel activity at whole cell configurations was measured in CFTR-expressing CHO cells with or without Shank2 co-transfection. Treatment with forskolin (3 μ M) evoked a large Cl⁻ current in mock-transfected cells (a), but not in Shank2-transfected cells (b). CFTR currents in Shank2-transfected cells were restored by treatment with the nonspecific PDE inhibitor 3-isobutyl-1-methylxanthine (IBMX) (b), or the PDE4-specific inhibitor, rolipram (d), but not with the PDE3-specific inhibitor, trequinsin (c). (e) Detection of PDE3 and PDE4 isoforms in NIH 3T3 cells (mouse fibroblast) and T84 cells (human colonic epithelia) by RT-PCR. Primer sequences specific to PDE3 and PDE4 isoforms were selected from the regions common to both mouse and human PDEs. (f) Expression of PDE4D proteins in NIH 3T3, CHO (Chinese hamster ovary), and T84 cells was analyzed by immunoblotting using anti-pan PDE4D ab14613. Several recombinant PDE4D splice variants are shown for comparison. (g) Shank2 and the PDE4D splice variant PDE4D5 were overexpressed in CHO cells (upper panels) and subsequently immunoprecipitated from cell extracts using anti-PDE4D5 (lower left panel) and anti-Shank2 (lower right panel) antibodies.

In order to identify its PDE4D-binding domain, several truncated Shank2 constructs were generated and used for pull-down assays. Shank2 has multiple sites for possible protein-protein interactions, including a PDZ domain, a long proline-rich (PR) region, and a SAM (sterile alpha motif) domain²⁰. The PR region contains five proline-rich clusters (PRCs), including a cortactin-binding domain (ppI). In initial pull-down assays using the lysates from the PDE4D5-transfected CHO cells, PDE4D5 showed an interaction with the PR region of Shank2 (FIG. 4b, left). The PR region was then further dissected into two parts, PR1 and PR2, and the PDE4D binding site was mapped to the PR2 region (FIG. 4b, right) where three PRCs and a ppI are clustered (FIG. 4a). Next, all PDE4D splice variants were coimmunoprecipitated with Shank2 in order to identify the PDE4D variants that interact with Shank2 and to identify the putative Shank2-binding site in PDE4D. COS-7 cells were transfected with plasmids encoding Shank2 and the nine PDE4D splice variants, PDE4D1 to PDE4D9, followed by immunoprecipitation using the PAN-PDE4D antibody, M3S1. All PDE4D long forms (D3, D4, D5, D7, D8, and D9) were found to interact with Shank2, whereas the short forms, D2 and D6, do not (FIG. 4d). A weak interaction was detected in the case of PDE4D1. The PDE4D splice variants are distinguished by the presence or absence of two conserved N-terminal domains called upstream conserved regions 1 and 2 (UCR1 and UCR2, FIG. 4c). The above results imply that UCR1 and the N-terminal part of UCR2 mediate Shank2 binding.

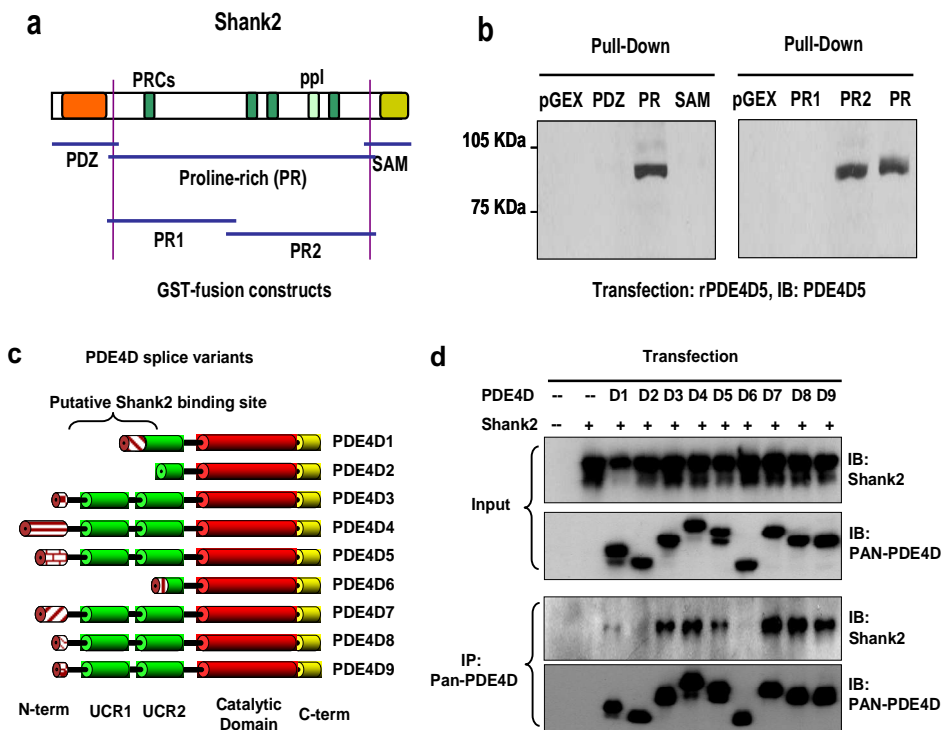


FIGURE 4. Domains responsible for the association between Shank2 and PDE4D (a,b) to identify the PDE4D-binding domain of Shank2, pulldown assays were performed using GST fusion proteins containing different domains of Shank2 and PDE4D expressed in CHO cells. Domain structures of the GST fusion proteins are illustrated in a, and pulldown results are shown in b. Lysates from rPDE4D5-transfected CHO cells were pulled down with GST-tagged Shank2 fragments and blotted with anti-PDE4D5 antibody. (c,d) Immunoprecipitation of Shank2 with the nine PDE4D splice variants. COS-7 cells were transfected with plasmids encoding Shank2 and the PDE4D splice variants, PDE4D1 to PDE4D9 (*D1–D9*). After 3 days of culture, cells were harvested, and the resulting detergent extracts were subjected to IP with the pan-PDE4D antibody M3S1. The domain structures of PDE4D splice variants are illustrated in c, and IP results are presented in d. *PRCs*, proline-rich clusters; *SAM*, sterile motif; *IB*, immunoblot.

4. Shank2 and PDE4D associate in vivo

The association between Shank2 and PDE4D was then examined in cells that natively express both proteins in order to explore its physiological role. Initially, I investigated the expression of Shank2 and PDE4D in rat colonic mucosa. Shank2 and PDE4D were highly co-localized at the apical region of colonic crypt cells where CFTR plays a major role in fluid and ion secretion (FIG. 5a). The Shank2-PDE4D interaction was also verified by immunoprecipitation of the endogenous proteins prepared from T84 human colonic epithelial cells. It is well known that PDE4 can be activated by PKA-induced phosphorylation at UCR1²². Interestingly, stimulation of the cAMP/PKA pathway using the adenylyl cyclase activator, forskolin, increased the physical association between Shank2 and PDE4D in T84 cells (FIG. 5b). Finally, the Shank2-PDE4D interaction was examined in mouse brain tissues where multiple PDE isoforms as well as Shank2 are expressed at high levels. In immunoprecipitates using PAN-PDE4D antibodies, multiple Shank2 immunoreactive bands were detected in addition to the typical 170 kDa Shank2 (FIG. 5c) due to the presence of distinct Shank2 splice variants in brain tissue. Mouse brain tissue was then immunoprecipitated with anti-Shank2 antibodies and the resulting IP pellets were subjected to PDE activity assays. The PDE activity coimmunoprecipitating with Shank2 was inhibited by the PDE4 selective inhibitor, rolipram (FIG. 5d). In addition, the co-immunoprecipitation of PDE was ablated in IPs using tissue from PDE4D knock-out mice (FIG. 5e) indicating that Shank2 specifically interacts with PDE4D in mouse brain tissue.

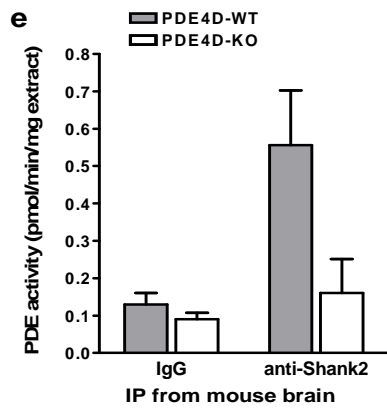
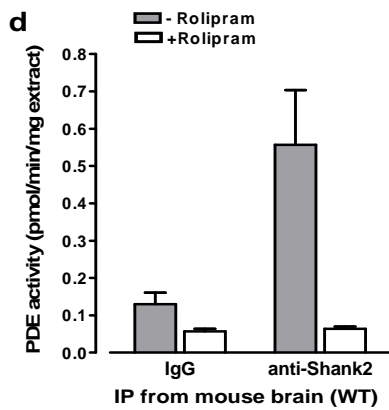
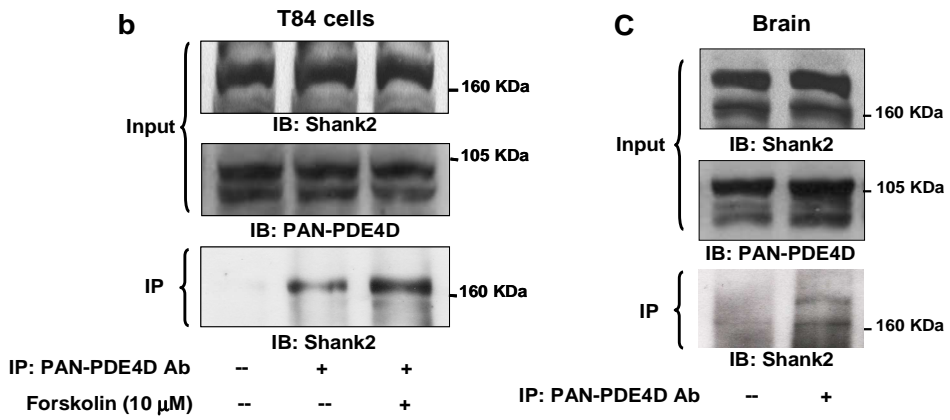
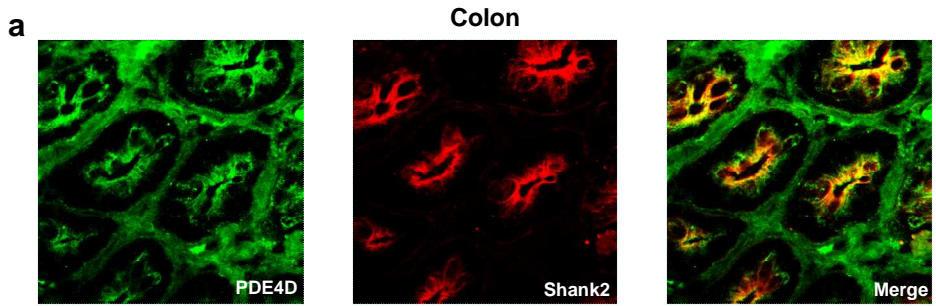


FIGURE 5. Shank2 and PDE4D associate *in vivo* (a) immunolocalization of Shank2 and PDE4D in rat colon was detected using polyclonal anti-Shank2 antibody 1136 and monoclonal pan-PDE4D antibody M3S1. Shank2 and PDE4D were co-localized in the apical region of colonic crypt cells. (b) co-IP of Shank2 and PDE4D from extracts of human colonic T84 cells. Forskolin treatment (10 μ M for 30 min) enhanced the association between Shank2 and PDE4D. (c) detection of Shank2 proteins in PDE4D immunoprecipitates from mouse brain. (d,e), measurement of PDE activity in Shank2 immunoprecipitates from mouse brain. In d, PDE activity in Shank2 IPs from wild type mice was determined in the presence or absence of the PDE4 specific inhibitor rolipram (10 μ M). In e, PDE activity in immunoprecipitates from PDE4D wild type mice (*PDE4D-WT*) is compared with immunoprecipitates from PDE4D knock-out mice (*PDE4D-KO*). *Ab*, antibody; *IB*, immunoblot.

IV. DISCUSSION

The regulatory mechanisms resulting from the association of CFTR with EBP50 and Shank2 are summarized in Figure 6. It is known that EBP50 can activate CFTR through two independent mechanisms. First, EBP50 can recruit ezrin, a PKA anchoring protein (AKAP), and hence facilitates the cAMP/PKA-mediated phosphorylation of CFTR⁶. Second, EBP50 can activate CFTR by conformational changes, possibly by forming a CFTR dimer¹⁵. The results of this study revealed that Shank2 can inhibit both mechanisms by competing with EBP50 at the C-terminus of CFTR. The finding that Shank2 inhibited the EBP50-induced increase of CFTR P_o in inside-out patches (Fig. 2) demonstrated that Shank2 can antagonize the EBP50 function by breaching the EBP50-induced active conformation of CFTR independent of cAMP signals. Even more interesting, this study shows that Shank2 can ablate cAMP signaling in the vicinity of the CFTR by tethering PDE4D into this macromolecular complex.

It is well known that cAMP signals are compartmentalized in many cell types, and that localized cAMP signals play a critical role in various physiological processes²⁴. For example, localized cAMP accumulation in a region overlapping with the Z band and the T tubules in cardiomyocytes is essential for the regulation of cardiac myocyte contraction by β -adrenergic receptors²². Several recent reports underscored the importance of PDE4D as a cAMP diffusion barrier formed at the apical membrane of epithelia for the proper functioning of CFTR^{18, 19}. However, the molecular mechanisms for PDE accumulation in apical regions remained obscure. A thorough molecular

characterization in this study revealed that the apical adaptor, Shank2, recruits PDE4D by a direct interaction between the proline-rich region of Shank2 and the UCR1/2 region of PDE4D. Recently, Shank2E, a splice variant of Shank2 with additional ankyrin repeats and an SH3 domain, was identified in epithelial cells²⁴. Therefore, I repeated the experiments in Figure 3 with Shank2E. The results were nearly identical to those obtained using Shank2 suggesting that domains within the structure of Shank2 are important for regulating CFTR function.

The physiological significance of the Shank2-PDE4D association is not confined to epithelial cells but can be extended to other organs. For example, Shank2 is widely expressed in many regions of the brain including cortex, hippocampus, and cerebellum. Shank proteins are the key organizer of PSD and interact with Homer^{20, 25}, which is required for efficient signaling of metabotropic glutamate receptors (mGluRs) that play a critical role in learning and memory. Effector systems of mGluRs are not only associated with Ca²⁺ signaling but also with cAMP signals, and it is believed that cAMP signals play a role in the functional specificity of each mGluR isoform^{27,28}. Therefore, Shank2-associated PDE4D may play a critical role in the regulation of PSD in neuronal cells.

Recent studies with knock-out animals of NHEFR family PDZ proteins (EBP50, E3KARP, and PDZK1) have shown that the functions of these adaptors are more complex than previously appreciated and appear to be tissue-specific⁵. Because PDZ domains have well-defined binding sites, they are promising targets for drug discovery²¹. However, as the present study demonstrates, much

is yet to learn about the function of each PDZ-based adaptor before drugs targeting PDZ interactions can become a reality²⁶. For example, as the PDZ structures of EBP50 and Shank2 are very similar, small molecules or peptides targeting EBP50 may have untoward effects *in vivo* by disrupting Shank2 complexes as well.

In conclusion, the present study demonstrates the functional diversity of PDZ-mediated protein-protein interactions and illustrates that opposite signals can be delivered to the same PDZ-binding motif of a given membrane protein by different adaptors. A competitive balance between the signal-conferring and signal-stopping PDZ interactions would be critical in the regulation of many membrane transporters and receptors, as demonstrated here for CFTR.

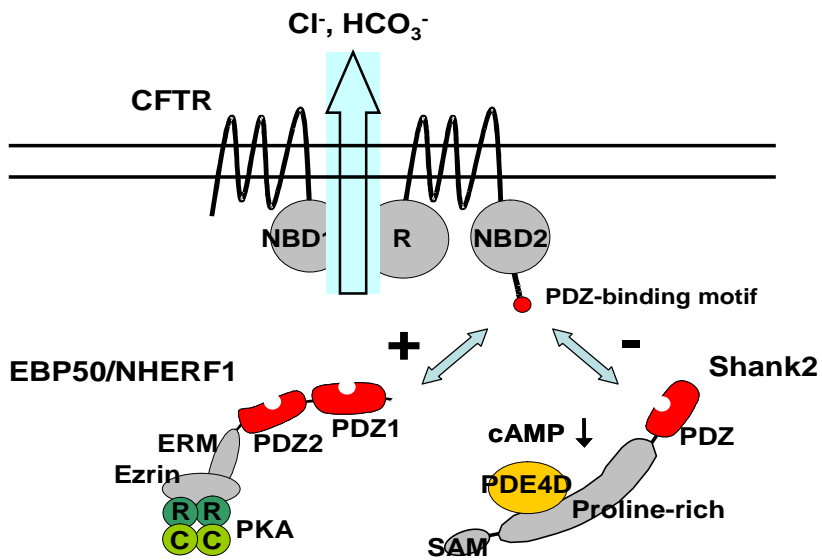


FIGURE 6. A model for the regulation of CFTR through interaction with EBP50 and Shank2 Through their respective PDZ domains, Shank2 and EBP50 compete for binding of the CFTR C terminus. Binding of EBP50 activates CFTR through a conformational change. In addition, EBP50 facilitates the PKA-mediated phosphorylation and activation of CFTR by bringing the AKAP ezrin and PKA into the protein complex. Shank2 inhibits CFTR activity by breaching the CFTR-EBP50 association and by bringing PDE4D, which precludes cAMP/PKA signaling, closer to CFTR. SAM, sterile α -motif; R of CFTR, R-domain; R and C of PKA, regulatory and catalytic subunits.

V. CONCLUSION

The present study shows the kinetic property and physiological significance of the interactions between CFTR and the PDZ-based scaffolds, EBP50 and Shank2. Using molecular, biophysical approaches, we conclude that:

1. The dissociation constant (KD) of CFTR-Shank2 binding was similar to that of CFTR-EBP50 binding, and that both proteins apparently compete for binding at the same site.
2. CFTR Cl⁻ channel activity was dynamically regulated by the competition of Shank2 and EBP50 binding.
3. Shank2 associates with PDE4D in vitro and vivo. UCR1 or UCR2 domain of PDE4D and latter Proline-Rich domain of Shank2 participate in interaction of PDE4D and Shank2, respectively.
4. In contrast to the PKA/AKAP-recruitment by EBP50, Shank2 was found to tether PDE4D to the CFTR complex, thus, attenuating cAMP/PKA signals.

These results strongly suggest that balanced interactions between the membrane transporters and multiple PDZ-based adaptors play a role in the homeostatic regulation of epithelial transport, and possibly the membrane transport in other tissues.

REFERENCES

1. Quinton PM. Physiological basis of cystic fibrosis: a historical perspective. *Physiol Rev.* 1999;79 Suppl 1:S3-S22.
2. Anderson MP, Rich DP, Gregory RJ, Smith AE, Welsh MJ. Generation of cAMP-activated chloride currents by expression of CFTR. *Science.* 1991;251:679-82.
3. Choi JY, Muallem D, Kiselyov K, Lee MG, Thomas PJ, Muallem S. Aberrant CFTR-dependent HCO₃⁻ transport in mutations associated with cystic fibrosis. *Nature.* 2001;410:94-7.
4. Chao AC, de Sauvage FJ, Dong YJ, Wagner JA, Goeddel DV, Gardner P. Activation of intestinal CFTR Cl⁻ channel by heat-stable enterotoxin and guanylin via cAMP-dependent protein kinase. *EMBO J.* 1994;13:1065-72.
5. Lamprecht G, Seidler U. The emerging role of PDZ adapter proteins for regulation of intestinal ion transport. *Am J Physiol Gastrointest Liver Physiol.* 2006;291:G766-77.
6. Donowitz M, Cha B, Zachos NC, Brett CL, Sharma A, Tse CM, et al. NHERF family and NHE3 regulation. *J Physiol.* 2005;567 (Pt 1):3-11.
7. Kim E, Sheng M. PDZ domain proteins of synapses. *Nat Rev Neurosci.* 2004;5:771-81.
8. Kim JY, Han W, Namkung W, Lee JH, Kim KH, Shin H, et al. Inhibitory regulation of cystic fibrosis transmembrane conductance regulator anion-transporting activities by Shank2. *J Biol Chem.* 2004;279:10389-96.

9. Han W, Kim KH, Jo MJ, Lee JH, Yang J, Doctor RB, et al. Shank2 associates with and regulates Na⁺/H⁺ exchanger 3. *J Biol Chem.* 2006;281:1461-9.
10. Weinman EJ, Steplock D, Wang Y, Shenolikar S. Characterization of a protein cofactor that mediates protein kinase A regulation of the renal brush border membrane Na⁽⁺⁾-H⁺ exchanger. *J Clin Invest.* 1995;95:2143-9.
11. Yun CH, Lamprecht G, Forster DV, Sidor A. NHE3 kinase A regulatory protein E3KARP binds the epithelial brush border Na⁺/H⁺ exchanger NHE3 and the cytoskeletal protein ezrin. *J Biol Chem.* 1998;273:25856-63.
12. Im YJ, Lee JH, Park SH, Park SJ, Rho SH, Kang GB, et al. Crystal structure of the Shank PDZ-ligand complex reveals a class I PDZ interaction and a novel PDZ-PDZ dimerization. *J Biol Chem.* 2003;278:48099-104.
13. Lim S, Naisbitt S, Yoon J, Hwang JI, Suh PG, Sheng M, et al. Characterization of the Shank family of synaptic proteins. Multiple genes, alternative splicing, and differential expression in brain and development. *J Biol Chem.* 1999;274:29510-8.
14. Richter W, Jin SL, Conti M. Splice variants of the cyclic nucleotide phosphodiesterase PDE4D are differentially expressed and regulated in rat tissue. *Biochem J.* 2005;388 (Pt 3):803-11.
15. Raghuram V, Mak DO, Foskett JK. Regulation of cystic fibrosis transmembrane conductance regulator single-channel gating by bivalent

- PDZ-domain-mediated interaction. *Proc Natl Acad Sci U S A*. 2001;98:1300-5.
16. Wang S, Yue H, Derin RB, Guggino WB, Li M. Accessory protein facilitated CFTR-CFTR interaction, a molecular mechanism to potentiate the chloride channel activity. *Cell*. 2000;103:169-79.
 17. Mehats C, Andersen CB, Filopanti M, Jin SL, Conti M. Cyclic nucleotide phosphodiesterases and their role in endocrine cell signaling. *Trends Endocrinol Metab*. 2002;13:29-35.
 18. Barnes AP, Livera G, Huang P, Sun C, O'Neal WK, Conti M, et al. Phosphodiesterase 4D forms a cAMP diffusion barrier at the apical membrane of the airway epithelium. *J Biol Chem*. 2005;280:7997-8003.
 19. Liu S, Veilleux A, Zhang L, Young A, Kwok E, Laliberte F, et al. Dynamic activation of cystic fibrosis transmembrane conductance regulator by type 3 and type 4D phosphodiesterase inhibitors. *J Pharmacol Exp Ther*. 2005;314:846-54.
 20. Sheng M, Kim E. The Shank family of scaffold proteins. *J Cell Sci*. 2000;113 (Pt 11):1851-6.
 21. Boeckers TM, Bockmann J, Kreutz MR, Gundelfinger ED. ProSAP/Shank proteins - a family of higher order organizing molecules of the postsynaptic density with an emerging role in human neurological disease. *J Neurochem*. 2002;81:903-10.
 22. Conti M, Richter W, Mehats C, Livera G, Park JY, Jin C. Cyclic AMP-specific PDE4 phosphodiesterases as critical components of cyclic AMP signaling. *J Biol Chem*. 2003;278:5493-6.

23. Zaccolo M, Pozzan T. Discrete microdomains with high concentration of cAMP in stimulated rat neonatal cardiac myocytes. *Science*. 2002;295:1711-5.
24. McWilliams RR, Gidey E, Fouassier L, Weed SA, Doctor RB. Characterization of an ankyrin repeat-containing Shank2 isoform (Shank2E) in liver epithelial cells. *Biochem J*. 2004;380 (Pt 1):181-91.
25. Tu JC, Xiao B, Naisbitt S, Yuan JP, Petralia RS, Brakeman P, et al. Coupling of mGluR/Homer and PSD-95 complexes by the Shank family of postsynaptic density proteins. *Neuron*. 1999;23:583-92.
26. Dev KK. Making protein interactions druggable: targeting PDZ domains. *Nat Rev Drug Discov*. 2004;3:1047-56.
27. Francesconi A, Duvoisin RM. Opposing effects of protein kinase C and protein kinase A on metabotropic glutamate receptor signaling: selective desensitization of the inositol trisphosphate/Ca²⁺ pathway by phosphorylation of the receptor-G protein-coupling domain. *Proc Natl Acad Sci U S A*. 2000;97:6185-90.
28. Tateyama M, Kubo Y. Dual signaling is differentially activated by different active states of the metabotropic glutamate receptor 1alpha. *Proc Natl Acad Sci U S A*. 2006;103:1124-8.

ABSTRACT (IN KOREA)

PDZ 연결 단백질에 의한 CFTR 기능 조절

지도교수 이 민 구

연세대학교 대학원 의과학과

이 지 현

염소이온을 비롯한 음이온 수송에 중요한 수송단백인 cystic fibrosis transmembrane conductance regulator (CFTR)의 기능이 과도하거나 감소될 경우 설사질환, 낭포성 섬유증 등 여러 질환을 일으킨다. CFTR 단백질의 발현과 기능 조절에는 PDZ-domain 을 갖고 있는 연결 단백질과의 결합이 중요한 역할을 한다고 알려져 있다. 예를 들어 CFTR 의 활성화에는 EBP50 라는 연결단백이 PKA 를 데리고 다니면서 CFTR 을 효율적으로 인산화시켜 CFTR 을 활성화한다고 알려져 있다. 반대로 불활성화 기전에는 Shank2 라는 연결 단백질이 관여한다고 알려져 있으나 아직 분자기전은 밝혀져 있지 않다.

본 연구에서는 EBP50 및 Shank2 에 의한 CFTR 조절의 분자기전을 규명하고자 하였다. 먼저 표면 플라즈몬 공명 (surface plasma resonance technology) 실험을 통해 EBP50 와 Shank2 단백질이 CFTR 의 C-말단에서 경쟁적으로 결합하고 있음을 발견하였다. 또한 single channel patch clamp 실험을 통하여 이런 Shank2 와 EBP50 의 경쟁적인 결합이 실제로 CFTR 의 이온통로 기능을 조절하고 있음을

확인하였다. 한편 Shank2 의 CFTR 억제 작용기전에 있어 PDE4D 가 결부되어 있는 것을 발견하였으며, Whole cell patch clamp 실험에서 PDE4 억제제가 Shank2 의 CFTR 억제 작용을 감소시키는 것을 하였다. 또한 면역침강법과 pull down 실험을 통해 Shank2 의 proline-rich 부위가 PDE4D 와의 결합에 중요한 역할을 하는 것을 확인하였으며, CFTR 이 물과 이온 수송에 중요한 역할을 한다고 알려진 대장세포에서도 Shank2 와 PDE4D 가 함께 발현함을 면역형광염색법을 이용하여 확인하였다.

이상의 결과를 바탕으로 EBP50 에 의한 CFTR 활성화 기전과 Shank2 에 의한 CFTR 불활성화 기전은 CFTR-C 말단에서 서로 상호 경쟁적으로 작용하고 있음을 발견하였으며 이는 인체 물-이온 항상성 유지에 중요한 역할을 하는 것으로 사료된다.

핵심되는 말: Cystic Fibrosis Transmembrane Conductance Regulator (CFTR), PDZ-based scaffolds, EBP50, shank2, PDE4, cAMP

PUBLICATION LIST

1. Choi JH, Ahn BM, Yi J, Lee JH, **Lee JH**, Nam SW, Chon CY, Han KH, Ahn SH, Jang IJ, Cho JY, Suh Y, Cho MO, Lee JE, Kim KH, Lee MG. MRP2 haplotypes confer differential susceptibility to toxic liver injury. *Pharmacogenet Genomics*. 2007;17:403-15.
2. **Lee JH**, Richter W, Namkung W, Kim KH, Kim E, Conti M, Lee MG. Dynamic regulation of cystic fibrosis transmembrane conductance regulator by competitive interactions of molecular adaptors. *J Biol Chem*. 2007;282:10414-22.
3. Han W, Kim KH, Jo MJ, **Lee JH**, Yang J, Doctor RB, Moe OW, Lee J, Kim E, Lee MG. Shank2 associates with and regulates Na⁺/H⁺ exchanger 3. *J Biol Chem*. 2006;281:1461-9.
4. Lee JE, Choi JH, **Lee JH**, Lee MG. Gene SNPs and mutations in clinical genetic testing: haplotype-based testing and analysis. *Mutat Res*. 2005;573:195-204.
5. Ahn KM, Park HY, **Lee JH**, Lee MG, Kim JH, Kang IJ, Lee SI. Cystic fibrosis in Korean children: a case report identified by a quantitative pilocarpine iontophoresis sweat test and genetic analysis. *J Korean Med Sci*. 2005;20:153-7.
6. Kim JY, Han W, Namkung W, **Lee JH**, Kim KH, Shin H, Kim E, Lee MG. Inhibitory regulation of cystic fibrosis transmembrane conductance regulator anion-transporting activities by Shank2. *J Biol Chem*. 2004;279:10389-96.

7. **Lee JH**, Choi JH, Namkung W, Hanrahan JW, Chang J, Song SY, Park SW, Kim DS, Yoon JH, Suh Y, Jang IJ, Nam JH, Kim SJ, Cho MO, Lee JE, Kim KH, Lee MG. A haplotype-based molecular analysis of CFTR mutations associated with respiratory and pancreatic diseases. *Hum Mol Genet.* 2003;12:2321-32.